Rock and Soil Mechanics

Volume 41 | Issue 4 Article 8

9-27-2020

A case study of excavation damage zone expansion time effect in hard brittle country rock under high geostress : characteristics and mechanism

Yan-shuang YANG
School of Civil Engineering and Construction, Hubei University of Technology, Wuhan, Hubei 430068, China

Hui ZHOU
State Key Laboratory of Geomechanics and Geotechnical Engineering, Institute of Rock and Soil Mechanics, Chinese Academy of Sciences, Wuhan, Hubei 430071, China, hzhou@whrsm.ac.cn

Song-hua MEI
Hunan Provincial Key Laboratory of Key Technology on Hydropower Development, Power China Zhongnan Engineering Corporation Limited, Changsha, Hunan 410014, China

Zhan-rong ZHANG
China Railway Siyuan Survey and Design Group Co., Ltd., Wuhan, Hubei 430063, China

See next page for additional authors

Custom Citation

YANG Yan-shuang, ZHOU Hui, MEI Song-hua, ZHANG Zhan-rong, LI Jin-lan, . A case study of excavation damage zone expansion time effect in hard brittle country rock under high geostress : characteristics and mechanism[J]. Rock and Soil Mechanics, 2020, 41(4): 1357-1365.

A case study of excavation damage zone expansion time effect in hard brittle country rock under high geostress : characteristics and mechanism

Authors
Yan-shuang YANG, Hui ZHOU, Song-hua MEI, Zhan-rong ZHANG, and Jin-lan LI

Rock and Soil Mechanics 2020 41(4): 1357−1365 ISSN 1000−7598
https: //doi.org/10.16285/j.rsm.2019.5020 rocksoilmech.researchcommons.org/journal

A case study of excavation damage zone expansion time effect in hard brittle country rock under high geostress：characteristics and mechanism

YANG Yan-shuang[1, 2], ZHOU Hui[3], MEI Song-hua[1], ZHANG Zhan-rong[4], LI Jin-lan[2]

1. Hunan Provincial Key Laboratory of Key Technology on Hydropower Development, Power China Zhongnan Engineering Corporation Limited, Changsha, Hunan 410014, China

2. School of Civil Engineering and Construction, Hubei University of Technology, Wuhan, Hubei 430068, China

3. State Key Laboratory of Geomechanics and Geotechnical Engineering, Institute of Rock and Soil Mechanics, Chinese Academy of Sciences, Wuhan, Hubei 430071, China

4. China Railway Siyuan Survey and Design Group Co., Ltd., Wuhan, Hubei 430063, China

Abstract: The excavation damage zone (EDZ) in hard brittle country rock exhibits noticeable time effect after excavation, as rock strength varies with time caused by the high geostress, which leads to the development of surrounding rock excavation damage zone and shows time-dependent characteristics. The LSSVM-PSO intelligent inversion analysis method considering time effect was established based on the time effect evolution model of rock strength, and measured EDZ data collected in the test tunnel of Jinping Ⅱ Hydropower Station, such as borehole monitoring, ultrasonic test and deformation monitoring were used as target functions. The orthogonal design method, least square support vector machine (LSSVM) model and principle of particle swarm optimization algorithm were used to simulate the EDZ's time effect evolution process between the time excavation ended and 25 days after in Jinping Ⅱ Hydropower Station. The study result shows: 1) Under high geostress, the principal geostress direction dominates the EDZ expanding, furthermore, the minimum principal stress direction is the main direction for EDZ extending and the failure zone (failure approach index, FAI≥2) also concentrates in this area. 2) The area of plastic zone after excavation develops to be "S" shaped curve. The area change of the plastic zone is relatively slow at beginning, then shows a linear increasing tendency and gradually becomes stabilized. 3) The plastic zone growth is rapidly increased from 3rd to 10th day after excavation, during which period rock burst is most likely to occur. The research results can provide guidance to the time effect characteristics of EDZ expanding in hard brittle surrounding rock mass under high geostress.

Keywords: excavation damage zone; failure approach index; time effect; intelligent inversion

1 Introduction

Numerous engineering practices and theoretical studies have shown that the development of excavation damage zone (EDZ) is critical to the safety of brittle hard rock tunnels [1−3]. Hao et al. [4] studied the displacement law of the excavation damage zone and found that the excavation damage zone of surrounding rock has a strong time effect. Li et al. [5] obtained the effect of excavation damage zone depth and deformation on the stability of surrounding rock by studying the columnar jointed rock mass. Chang et al. [6] developed a damage model based on laboratory experiments and used Fish to apply it to the excavation damage zone simulation. In the alpine valley area, due to the influence of high stress, the strength of the rock material will further deteriorate over time after the tunnel is excavated, which will inevitably lead to the development of tunnel excavation damage zone with significant time effect.

At present, in the study of tunnel excavation damage zone, there are few studies on the time-dependent evolution law of excavation damage zone. In addition, the research object is mainly shallow buried tunnels. There are very few studies on deep buried tunnels at more than 2000 m. Thirdly, the study of the damage zone mainly considers the excavation shape of tunnel in space, and does not consider the time-dependent characteristics of excavation damage zone caused by the weakening of the rock mass mechanical parameters with time under high stress conditions.

In this context, this study established the least squares support vector machines–particle swarm optimization (LSSVM–PSO) intelligent inversion analysis method considering time effect based on the time-dependent evolution model of rock strength and the test results of excavation damage area, such as borehole camera, acoustic wave and

Received: 7 January 2019 Revised: 26 July 2019
This work was supported by the National Natural Science Foundation of China (51609080, 51504089) and the Open Research Fund of Hunan Provincial Key Laboratory of Hydropower Development Key Technology (PKLHD201403).
First author: YANG Yan-shuang, female, born in 1984, PhD, Lecturer, research interests: time-dependent theories of deep ground hard brittle rock.
E-mail: y1y1s1@qq.com
Corresponding author: ZHOU Hui, male, born in 1972, PhD, Professor, research interests: rock mechanics experiments, theoretical and numerical analysis and engineering safety. E-mail: hzhou@whrsm.ac.cn

deformation monitoring from the test tunnel of Jinping II hydropower station, with orthogonal design method, least squares support vector machine model, particle swarm optimization algorithm and other methods. The evolution process of excavation damage zone of the Jinping II hydropower station test tunnel was studied and analyzed, with a time span from the tunnel excavation completion and the following 25 days. The time-dependent expansion characteristics of excavation damage zone due to the time-dependent rock strength evolution under high stress conditions were mainly studied.

2 LSSVM-PSO intelligent inversion analysis method considering the time-dependent expansion of excavation damage zone

The time-dependent expansion of surrounding rock excavation damage zone is based on the time-dependent evolution of rock mass strength under high stress conditions. To investigate the time-dependent expansion process of surrounding rock mass excavation damage zone, it is necessary to study the time-dependent evolution law of surrounding rock strength under different load conditions based on the time-dependent evolution model of rock strength, so as to obtain the time-dependent expansion characteristics of excavation damage zone.

2.1 Time-dependent evolution model of rock strength[8]

During the damage process of brittle hard rock, its time-dependent strength evolution has certain regularities: (i) External loads beyond a certain level will damage the rock interior and reduce the rock strength. (ii)The damage rate of rock strength depends on the loading magnitude, the greater the load, the faster the rock strength decreases. Therefore, the strength of brittle hard rock at a certain moment is characterized by the cohesion c and internal friction angle φ of the rock at given time, and the evolution rates of c and φ are related to the initial strength of rock and the yield approach index YAI [9−10], as following formula:

$$\left.\begin{aligned}
&\frac{\mathrm{d}c}{\mathrm{d}t}=-\alpha_1\left(\mathrm{e}^{\alpha_2(1-\mathrm{YAI})}-1\right)\\
&\frac{\mathrm{d}\varphi}{\mathrm{d}t}=\beta_1\left(\mathrm{e}^{\beta_2(1-\mathrm{YAI})}-1\right)\\
&\mathrm{YAI}\Big|_{\text{M−C Criterion}}=1-\frac{(I_1\sin\varphi)/3+(\cos\theta_\sigma-\sin\theta_\sigma\sin\varphi/\sqrt{3})\sqrt{J_2}-c\cos\varphi}{I_1\sin\varphi/3-c\cos\varphi}\\
&c\big|_{t=0}=c_0\\
&\varphi\big|_{t=0}=\varphi_0
\end{aligned}\right\} \tag{1}$$

where α_1, α_2, β_1 and β_2 are model parameters, which can be obtained through comprehensive field tests and optimization algorithms, and are constants. The initial cohesive force c_0 and initial internal friction angle φ_0 are the strength parameters of the rock in its initial state. t is the time starting from the excavation of rock mass. YAI is the relative ratio of the rock stress state to the safest stress state in the stress space. The YAI in this paper is based on the Mohr-Coulomb strength criterion.

2.2 Inverse analysis method based on time-dependent evolution model of rock strength

The time-dependent based inverse analysis method is on the basis of the time-dependent evolution model of rock strength. Actual monitoring data from the measured excavation deformation and damage zones are used. The analysis plan is determined based on the orthogonal design method and the numerical analyses are conducted item by item. Predetermined calculation parameters and corresponding calculation values as learning samples are combined with least squares support vector machines (LSSVM）regression algorithm to determine the mapping relationship between the parameters in the time-dependent evolution model of rock strength and rock deformation and the range of excavation damage zone.

2.2.1 Orthogonal test design

The orthogonal test design method is based on the principle of orthogonality and mathematical statistics. The orthogonal test table is used to select representative test parameters and the law analysis for calculation results are performed instead of analyzing all test parameters. The frequency of selected representative parameters is low and can reflect the objective change law of the test results, which effectively reduces the calculation amount. This paper analyzes the relationship between the parameters of rock time-dependent model and the measuring points deformation and damage zone. That is, the orthogonal test design method is used to construct the mapping relationship of the least square support vector machine model.

2.2.2 Least square support vector machine

Least square support sector machine(LSSVM)[11] is a regression analysis method. It assumes that $x_i \in R^n$ and $y_i \in R$ are the output values corresponding to the dimensional vector n respectively, then the linear function of the fitted data of the optimal solution for training sample $\{x_i, y_i\}$, (i = 1，2，…，k) is

$$f(x)=\boldsymbol{w}\varphi(x)+\boldsymbol{b} \tag{2}$$

where $\boldsymbol{w}$ is the weight vector and $\boldsymbol{b}$ is the offset. This linear

function maps the training samples to the *n* dimensional feature space $\varphi(x_i)$. The loss function is defined as the second norm of the error ξ_i, and then the objective function of LSSVM optimization problem is obtained, thus the inequality constraint of the standard support vector machines (SVM) is converted into the equality constraint, that is

$$\min_{w,b,\xi} \frac{1}{2}\|\boldsymbol{w}\|^2 + C\frac{1}{2}\sum_{i=1}^{k}\xi_i^2 \tag{3}$$

The restrictions are

$$y_i - \boldsymbol{w}\varphi(x_i) = \boldsymbol{b} + \xi_i \tag{4}$$

The adjustment constant $\boldsymbol{C}$ is introduced to obtain the Lagrange equations of Eqs. (3) and (4) and to improve the generalization of Eq. (2).

$$L(\boldsymbol{w},\boldsymbol{b},\boldsymbol{\xi},\boldsymbol{a}) = \frac{1}{2}\|\boldsymbol{w}\|^2 + \boldsymbol{C}\sum_{i=1}^{k}\boldsymbol{\xi}_i^2 - \sum_{i=1}^{k}a_i[\boldsymbol{w}\varphi(x_i) + \boldsymbol{b} + \xi_i - y_i] \tag{5}$$

where a_i（$i = 1$，2，…，k）is the Lagrange multiplier. The optimal solutions of $\boldsymbol{a}$ and $\boldsymbol{b}$ can be obtained by deriving the extremum:

$$\left.\begin{aligned} &\frac{\partial L}{\partial \boldsymbol{b}} = 0 \Rightarrow \sum_{i=1}^{k} a_i = 0 \\ &\frac{\partial L}{\partial \boldsymbol{\xi}} = 0 \Rightarrow a_i = \boldsymbol{C}\xi_i \\ &\frac{\partial L}{\partial \boldsymbol{w}} = 0 \Rightarrow \boldsymbol{w} = \sum_{i=1}^{k} a_i\varphi(x_i) \\ &\frac{\partial L}{\partial \boldsymbol{w}} = 0 \Rightarrow \boldsymbol{w} = \sum_{i=1}^{k} a_i\varphi(x_i) \end{aligned}\right\} \tag{6}$$

After simplification of $\boldsymbol{w}$ and ξ, optimization problems are transformed into

$$\begin{bmatrix} 0 & \boldsymbol{\Theta}^{\mathrm{T}} \\ \boldsymbol{\Theta} & \boldsymbol{\Omega} + \boldsymbol{C}^{-1}\mathbf{I} \end{bmatrix}\begin{bmatrix} \boldsymbol{b} \\ \boldsymbol{a} \end{bmatrix} = \begin{bmatrix} 0 \\ \boldsymbol{y} \end{bmatrix} \tag{7}$$

where $\boldsymbol{y} = [y_1, y_2, \ldots, y_k]^{\mathrm{T}}$; $\boldsymbol{a} = [a_1, a_2, \ldots, a_k]^{\mathrm{T}}$ and $\boldsymbol{\Theta} = [1, \ldots, 1]^{\mathrm{T}}$; $\boldsymbol{\Omega}$ is a square matrix, $\boldsymbol{\Omega}_{i,j} = \varphi(x_i)^{\mathrm{T}}\varphi(x_j)$ is the data in the *i*-th row and *j*-th column. The symmetric function $K(x_i, x_j)$ that satisfies the Mercer condition is a kernel function. $K(x_i, x_j)$ is generally a linear function. The inner product of the sample space is replaced by its kernel function, i.e. $K(x_i, x_j) = \varphi(x_i)\varphi(x_j)$, and thus the values of $\boldsymbol{a}$ and $\boldsymbol{b}$ and the regression model expression of LSSVM are obtained as:

$$f(x) = \sum_{i=1}^{k} a_i K(x_i, x_i) + \boldsymbol{b} \tag{8}$$

The value selection of adjustment constant $\boldsymbol{C}$ and the kernel function are the key factors that affect the accuracy of the LSSVM regression model. The values of the two are determined by the particle swarm optimization algorithm.

2.2.3 Particle swarm optimization algorithm

Particle swarm optimization (PSO)[12] is an optimization algorithm based on the iterative principle. It uses particles in space as the solution to optimization problem. The adjustment value of the particles is determined by the optimized function. By assigning a moving speed value to adjust the position of the particles in space, the particle speed is adjusted in the solution space in combination with the current optimal position. That is, a group of initial particles is randomly generated, iterative analysis is used to continuously obtain the optimal position of the particles, and the particles adjust the spatial position according to the individual and global optimal values during iteration. The best individual value is the optimal solution of each particle in each iteration analysis, and the global best value $\boldsymbol{g}_{\mathrm{best}}$ is the optimal solution of all particles in each iteration analysis. Assuming that the particle swarm is located in *n* dimensional space, $\boldsymbol{x}_i = (x_{i1}, x_{i2}, \ldots, x_{in})$, $\boldsymbol{v}_i = (v_{i1}, v_{i2}, \ldots, v_{in})$ and $\boldsymbol{P}_{\mathrm{best}} = (P_{i1}, P_{i2}, \ldots, P_{in})$ represent the spatial position, moving speed value, and monomer excellent value of the *i*-th particle, respectively, and $\boldsymbol{g}_{\mathrm{best}} = (g_1, g_2, \ldots, g_n)$ represents the global best value of the entire particle group. By adopting the iterative analysis, the individual best value of each particle and the global best value of the particle group are obtained to adjust the speed and position of each particle.

$$\left.\begin{aligned} &\boldsymbol{v}_i(k+1) = m\boldsymbol{v}_i(k) + \\ &c_1\mathrm{rand}_1(\boldsymbol{P}_{\mathrm{best}} - \boldsymbol{x}_i(k)) + c_2\mathrm{rand}_2(\boldsymbol{g}_{\mathrm{best}} - \boldsymbol{x}_i(k)) \\ &\boldsymbol{x}_i(k+1) = \boldsymbol{x}_i(k) + \boldsymbol{v}_i(k+1) \end{aligned}\right\} \tag{9}$$

where c_1 and c_2 denote the adjustment parameters, respectively, and the value interval is (0, 2); ran d_1 and ran d_2 are the random variable, the value interval is (0, 1); *m* is the speed coefficient, and its value is continuously adjusted during the iterative analysis process.

2.2.4 Inverse analysis models of LSSVM and PSO

(1) LSSVM inverse analysis model

Determine *k* sets of training sample data according to the orthogonal test, which are $\{x_i, y_i\}$ $(i = 1, 2, \ldots, k)$, where $x_i \in R^n$ are the parameters to be inverted, $y_i \in R$ are the corresponding featured point deformation and damage zone range. A nonlinear mapping relationship is established between the to-be-inverted parameters and the range of rock mass deformation and damage zone.

$$f: R^n \to R \tag{10}$$

$$y_i = f(x_i) \quad (i = 1, 2, \ldots, k) \tag{11}$$

The model is established according to the process of finding the above relationship. That is, the inverse analysis model is established according to the LSSVM theory.

$$f(x) = \sum_{i=1}^{k} a_i K(x, x_i) + \boldsymbol{b} \tag{12}$$

$\boldsymbol{a}$ and $\boldsymbol{b}$ are solved according to Eq. (5). The kernel function is defined as the radial basis kernel function, and the PSO algorithm is used to search for the optimal adjustment constant $\boldsymbol{C}$ and kernel function.

Based on the above analysis model, the PSO algorithm is used in the global space to iteratively search for the inversion

parameters to obtain the optimal solution of the inversion parameters. That is, to ensure that the predicted values of the deformation and damage zone ranges are closest to the actual monitoring test values. In order to improve the accuracy during the analysis, multiple monitoring target values are generally selected, such as the deformation of the typical position and the actual test value of the typical test hole in damage zone, thus to determine the optimal solution of the inversion parameters. The target function is the sum of squares of the difference between the measured values and the calculated value of the target value:

$$F(\boldsymbol{X}) = \sum_{i=1}^{n} [f_i(\boldsymbol{X}) - y_i]^2 \quad (13)$$

where $\boldsymbol{X} = (x_1, x_2, ..., x_k)$ is a group of parameters to be determined by inverse analysis. $f_i(\boldsymbol{X})$ and y_i are the calculated values and measured values of i parameters; n is the number of inverse analysis parameters.

(2) Steps of inverse analysis

PSO-LSSVM inverse analysis flow chart is shown in Fig.1. The analysis process is as follows:

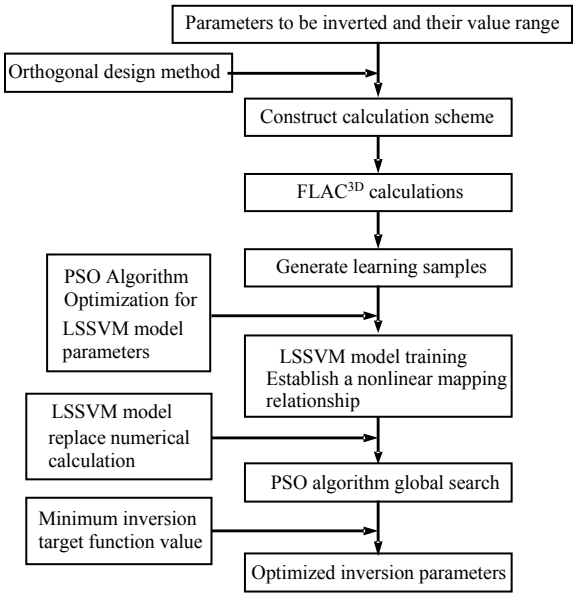

Fig.1 Inverse analysis flow chart of LSSVM and PSO

1) Determine the number and range of inverse analysis parameters based on engineering experience or test data, and determine the number of analyses based on orthogonal test design.

2) Establish LSSVM model learning samples: take the parameter vector to be inverted x_i as input, and use the time-dependent evolution model of brittle hard rock strength to calculate each group of input vectors, and output the calculated characteristic point deformation and characteristic damage area of each scheme y_i.

3) Initial setting of PSO optimization algorithm, including particle swarm size, planned number of iterations, adjustment parameters, initial random particle swarm vector, adjustment constant $\boldsymbol{C}$ and kernel function of each particle vector corresponding to LSSVM model. The learning samples are used as mutual verification samples at the same time. Substituting the individual best value of each particle into the LSSVM model to learn and to obtain the predicted values of characteristic point deformation and the characteristic damage zone of each corresponding sample.

4) The relative error between the actual value and the predicted value of each particle is used as the adjustment value to perform iterative analysis and calculation. Adjust the speed and orientation of the particle, and compare the optimal adjustment value between the individual particle and the group until the maximum number of iterations, which is the optimal inversion value $(\boldsymbol{C}, \sigma^2)$.

5) The best parameters obtained by iterative analysis using the PSO optimization method are input into the LSSVM model to obtain the relationship between the parameters to be inverted and the deformation of characteristic points and the range of characteristic damage zone.

6) Determination of optimal inversion parameters. When the inversion parameters are input into the LSSVM model, the corresponding deformation and the damage zone range of the specific location can be obtained. Therefore, the LSSVM model can replace the finite element model to analyze the time effect of surrounding rock strength. In order to determine the optimal inversion parameters, the adjustment parameters of particles are taken as the objective function values of LSSVM model, that is, PSO method is used to search the inversion parameters globally, and a group of parameters to be inversed with the minimum error with the measured values of deformation of characteristic points and damage zone of characteristic areas are obtained, which are the optimal inversion parameters

3 Analysis of engineering examples

3.1 Engineering background and field test results of excavation damage zone

The Jinping II hydropower station is located on the main stream of the Yalong River in the Liangshan Yi autonomous prefecture of Sichuan province. A total of seven large buried tunnels are arranged in parallel. From north to south, there are four parallel diversion tunnels #1, 2#, 3# and 4#, construction drainage tunnel and auxiliary tunnels B and A . The diversion tunnels pass under Jinping mountain. The average length of the diversion tunnel is about 17 km, the diameter of the excavated tunnel is 12.4 to 13.0 m, the diameter of the tunnel after support and reinforcement is 11.8 m, and the maximum buried depth is 2525 m. The tunnel have the characteristics of long tunnel, deep excavation and large size,

After the tunnel is excavated, the high ground stress causes the mechanical properties of rock mass to decrease, the mechanical parameters of the rock mass to deteriorate. The

deformation of the rock mass in the excavation damage zone will continue to develop. As a result, the scope of excavation damage zone gradually expands with time. Figure 2 is the layout of test tunnel F of Jinping hydropower station. During the excavation process of test tunnel F, the deformation is monitored during the construction period. In addition, a series of monitoring was performed including on-site sound wave tests and borehole camera tests before and after the test tunnel excavation. This article is based on this engineering case.

The main test results on site are as follows [7]: (i) In the initial stage of tunnel excavation, the evident deformation areas were mainly concentrated within a range of about 4 m from the excavation area. With the passage of time, the rock mass was significantly affected by the excavation at distance of 6m from excavation area (the hole depth is 17 m) after the deformation of the auxiliary tunnel was stabilized, and the deformation was significantly larger than the deep rock mass, which can be determined as the surrounding rock damage zone. (ii) The maximum deformation value of the test hole end is about 2.3 mm, and it occurred at the side wall. (iii) From the excavation on December 23, 2009 to January 12, 2010, which lasted about 20 days, the excavation damage zone of the test tunnel F no longer expanded. This article will combine the above measured data to study the time-dependent evolution characteristics of the tunnel surrounding rock excavation damage zone.

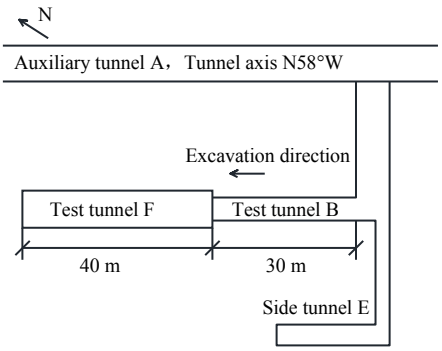

Fig.2 The test tunnel location and profile

3.2 Sample structure

The known mechanical parameters of marble in the test tunnel F of Jinping II hydropower station are shown in Table 1. The six parameters in the rock strength time-dependent evolution model are keys to determine the time-dependent expansion characteristics of the surrounding rock excavation damage zone. In order to reduce the workload of parameter inversion analysis and reduce the analysis difficulty, α_1, α_2, β_1 and β_2 are limited according to the nature of the rock material. The value ranges of c_0 and φ_0 are adjusted appropriately based on reference [8]. The specific parameter ranges are: α_1=0.002 0–0.064 0, α_2=0.000 5–0.032 0, β_1=0.000 5–0.032 0, β_2=0.000 5–0.032 0, c_0 = 16–32 MPa and φ_0=16°–32°. For orthogonal test analysis, five sets of calculation samples are constructed, as shown in Table 2.

Table 1 The rock mass mechanical parameters

γ/(kN·m^{-3})	E/GPa	μ	R_t/MPa	C_r/MPa	φ_r/(°)	ψ/(°)
26.3	25.3	0.22	1.5	3.1	46	10

Note: γ is the unit weight; E is the Young's modulus; μ is the Poisson's ratio; R_t is the tensile strength; C_r is the residual cohesion; φ_r is the residual friction angle; and ψ is the dilation angle.

Table 2 The coefficients of inverse analysis

Level	α_1	α_2	β_1	β_2	c_0/MPa	φ_0/(°)
1	0.002	0.000 5	0.000 5	0.000 5	16	16
2	0.008	0.002 0	0.002 0	0.002 0	20	20
3	0.016	0.008 0	0.008 0	0.008 0	24	24
4	0.032	0.016 0	0.016 0	0.016 0	30	30
5	0.064	0.032 0	0.032 0	0.032 0	32	32

According to the principle of orthogonal test design, the orthogonal test table L25 (56) with 6 factors and 5 levels is selected. Table 3 gives a scheme of 25 test combination groups. Based on the time-dependent evolution model of rock strength, FLAC^{3D} is used to calculate each set of test data to obtain the deformation value D of the test hole end, and the range value L of the excavation damage zone along the direction of the test hole 20 days after the excavation is completed. The corresponding input parameters are combined to obtain 25 sets of learning samples to train the LSSVM and PSO inverse analysis models.

Table 3 The parameter combination of orthogonal test scheme and the calculated deformation of each monitoring hole

Combination	α_1	α_2	β_1	β_2	c_0/MPa	φ_0/(°)	D/mm	L/m
1	0.002 0	0.000 5	0.000 5	0.000 5	16	16	3.53	14.5
2	0.002 0	0.002 0	0.002 0	0.002 0	20	20	3.15	9.6
3	0.002 0	0.008 0	0.008 0	0.008 0	24	24	2.77	7.9
4	0.002 0	0.016 0	0.016 0	0.016 0	30	30	2.29	5.4
5	0.002 0	0.032 0	0.032 0	0.032 0	32	32	2.18	4.6
6	0.008 0	0.000 5	0.002 0	0.008 0	30	32	2.18	4.6
7	0.008 0	0.002 0	0.008 0	0.016 0	32	16	3.54	14.5
8	0.008 0	0.008 0	0.016 0	0.032 0	16	20	3.15	9.6
9	0.008 0	0.016 0	0.032 0	0.000 5	20	24	2.77	7.9
10	0.008 0	0.032 0	0.000 5	0.002 0	24	30	2.29	5.4
11	0.016 0	0.000 5	0.008 0	0.032 0	20	30	2.29	5.4
12	0.016 0	0.002 0	0.016 0	0.000 5	24	32	2.18	4.6
13	0.016 0	0.008 0	0.032 0	0.002 0	30	16	3.53	14.5
14	0.016 0	0.016 0	0.000 5	0.008 0	32	20	3.14	9.6
15	0.016 0	0.032 0	0.002 0	0.016 0	16	24	2.77	7.9
16	0.032 0	0.000 5	0.016 0	0.002 0	32	24	2.77	8.2
17	0.032 0	0.002 0	0.032 0	0.008 0	16	30	2.29	5.4
18	0.032 0	0.008 0	0.000 5	0.016 0	20	32	2.18	4.6
19	0.032 0	0.016 0	0.002 0	0.032 0	24	16	3.53	14.5
20	0.032 0	0.032 0	0.008 0	0.000 5	30	20	3.14	9.6
21	0.064 0	0.000 5	0.032 0	0.016 0	24	20	3.14	9.6
22	0.064 0	0.002 0	0.000 5	0.032 0	30	24	2.77	8.2
23	0.064 0	0.008 0	0.002 0	0.000 5	32	30	2.29	5.4
24	0.064 0	0.016 0	0.008 0	0.002 0	16	32	2.18	4.6
25	0.064 0	0.032 0	0.016 0	0.008 0	20	16	3.54	14.5

3.3 Inversion results

According to the field test results, the deformation value of the test hole end at 20 days after the excavation completion of 2.3 mm and the range of the excavation damage zone along the test hole of 6 m are as the target object. The inverse analysis of the aforementioned method is used to obtain the time-dependent rock strength evolution model parameters, as shown in Table 4.

Table 4 Results of inverse analysis

α_1	α_2	β_1	β_2	c_0/MPa	φ_0/(°)
0.015 1	0.002 3	0.004 3	0.001 9	25.7	20.5

In order to verify the correctness of the LSSVM-PSO intelligent inversion analysis method, the inversion parameters are substituted into FLAC^{3D} to calculate the test hole deformation value and the range of excavation damage zone along the direction of test hole, which are defined as the calculated values. At the same time, the corresponding predicted values are obtained by extrapolating the inversion parameter value. Table 5 lists the calculated value, the predicted value and the measured value, and the three basically agree, indicating that the LSSVM-PSO intelligent inversion analysis method considering the time-dependent expansion of the excavation damage zone has good reliability.

Table 5 Comparison of monitoring value, forward calculation value of inversion parameter and LSSVM-PSO extrapolation predictive value

Method	Deformation/mm	Damage zone/m
Measured value	2.3	6.0
Calculated value	2.4	5.4
Predicted value	2.2	6.3

3.4 Time-dependent evolution characteristics of surrounding rock excavation damage zone

The time-dependent expansion characteristics of surrounding rock excavation damage zone is further analyzed, and the plastic zone range is used to describe the expansion range of surrounding rock excavation damage zone. Figure 3 shows the corresponding excavation damage zone at the excavation completion of test tunnel and at 1, 3, 5, 7, 10, 13, 19, and 25 days after excavation completion. Combined with the actual situation of the test tunnel F (Fig. 4), the evolution law of damage zone at different positions in the cross section was analyzed.

Figure 5 presents the variation curves of the excavation damage zone range with time in 8 different areas such as the vault, the left and right walls and the center line of the floor.

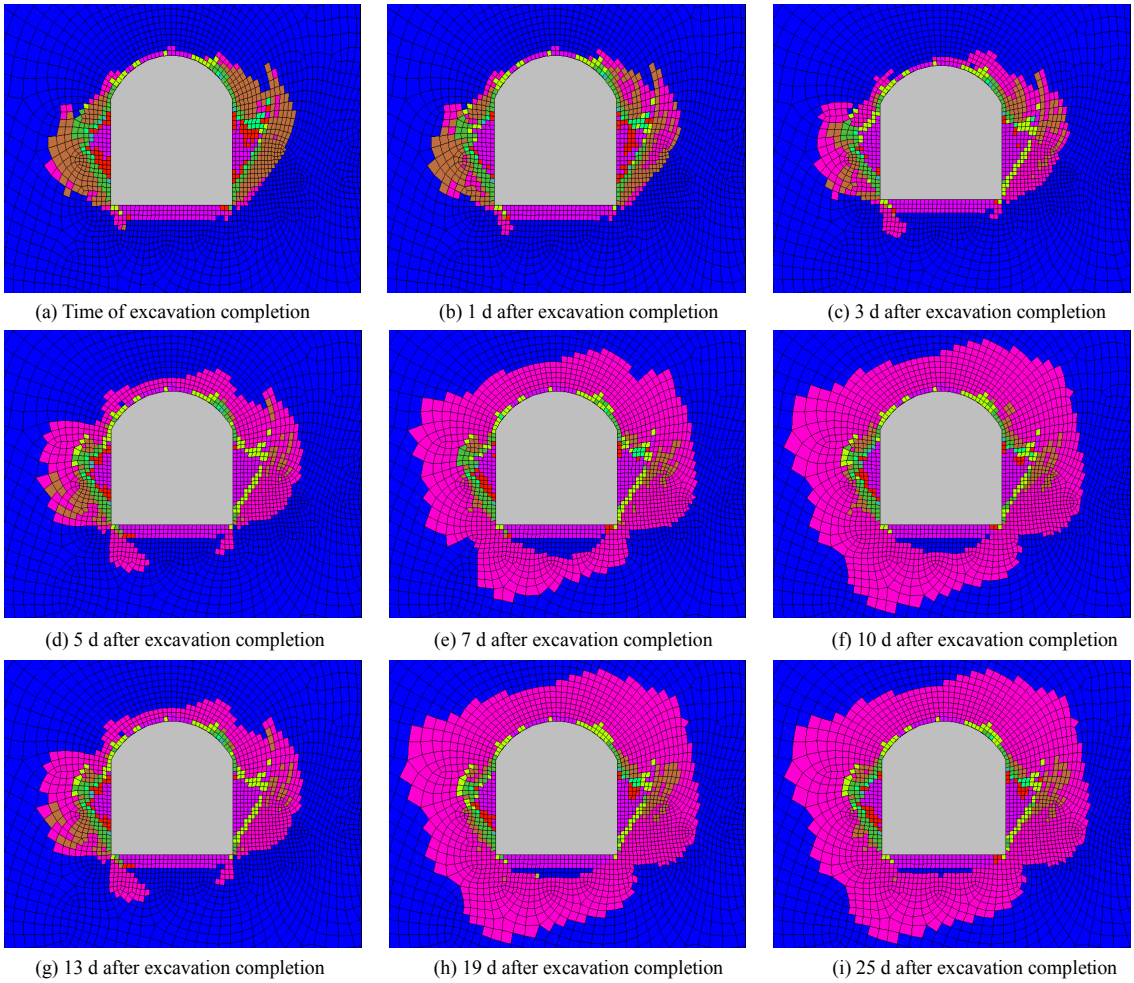

(a) Time of excavation completion (b) 1 d after excavation completion (c) 3 d after excavation completion

(d) 5 d after excavation completion (e) 7 d after excavation completion (f) 10 d after excavation completion

(g) 13 d after excavation completion (h) 19 d after excavation completion (i) 25 d after excavation completion

Fig.3 The damage zone range diagram of surrounding rock at different times after excavation

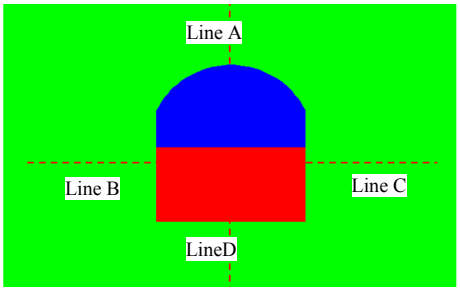

Fig.4 Position diagram of damage zone research line

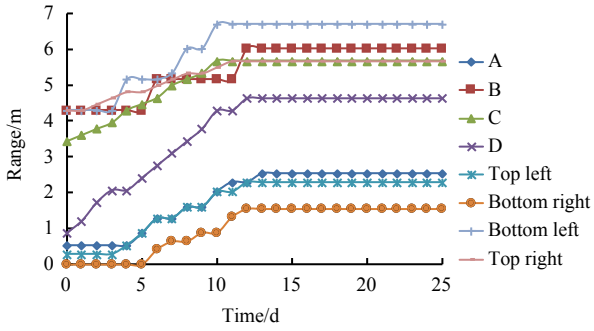

Fig.5 Variation of surrounding rock damage zone range with time after excavation

The excavation damage zone of surrounding rock is 3 to 5 m when the excavation is completed, but the vault and floor areas are controlled by the maximum principal stress, and the damage area range is only around 1 m (Fig.3(a)). As time elapses, the area of damage zone continues to expand and approximates a linear developing trend. About 12 days after the completion of the test tunnel excavation, the range of damage zone tends to be stable. The damage zone of centerline of the vault, left wall, right wall, and floor is analyzed. The final stable ranges are about 2.5, 6, 5.7, and 4.6 m, respectively, and the range of excavation damage zone at the test tunnel is basically consistent with the aforementioned monitoring data (Figs.(g)−(i)). In addition, the maximum principal stress of tunnel is slightly to the upper left part. After the excavation is completed, the shape of excavation damage zone has been presented approximately as an inclined rectangle. The inclined direction is approximately the principal stress direction, and the expansion of damage zone in the direction of minimum principal stress is significantly greater than in the direction of the maximum principal stress, which indicates that in the area of high geostress, the expansion direction of the surrounding rock excavation damage zone after tunnel excavation is controlled by the principal stress, and the maximum expansion direction is the direction of the minimum principal stress. This conclusion is consistent with field test data.

Figure 6 shows the change of excavation damage zone area with time, which is approximated as a S-shaped curve. The initial development is relatively slow, and it tends to increase linearly with time, and finally stabilizes gradually. To a certain extent, it can be explained that after the energy is released duo to excavation and unloading, the surrounding rock will enter a relatively quiet period. As the internal damage of surrounding rock accumulates, the area of surrounding rock damage will expand rapidly, and finally reach a relative equilibrium state and stabilize. This indicates that there are initial deformation period, acceleration period and stable periods in the excavation damage zone.

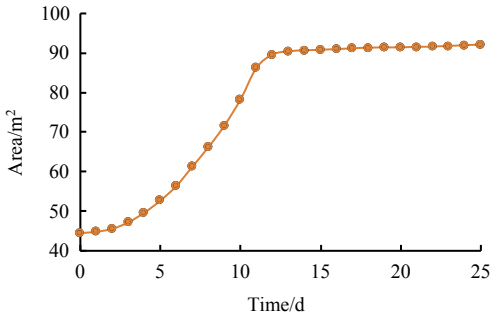

Fig.6 Variation of the damage zone area of surrounding rock with time after excavation

3.5 Analysis of time-dependent evolution characteristics of FAI

Failure approach index is the degree to which a material or structure approaches or reaches yield failure in the most unfavorable manner under load, and its calculation formula is [10]

$$\mathrm{FAI}=\begin{cases}\omega & ,0\leqslant\omega\leqslant 1\\ 1+FD & ,\omega=1,FD\geqslant 0\end{cases} \tag{12}$$

where $FD=\overline{\gamma}/\overline{\gamma}$, $\overline{\gamma}_{\mathrm{p}}$ is the equivalent plastic shear strain, $\overline{\gamma}_{\mathrm{p}}^{\mathrm{r}}$ is the material's ultimate equivalent plastic shear strain; ω is the complementary parameter of yield proximity, ω=1−YAI, YAI is the yield approach index as equation (1).

The failure approach index FAI is further used to describe the time evolution characteristics of surrounding rock damage zone. Figure 7 lists the FAI distribution range of test tunnel when the excavation is completed and 1, 3, 5, 7, 10, 13, 19, and 25 days after the excavation completion.

Figure 7 presents that the distribution of FAI is also controlled by the in-situ stress field. When the test tunnel is excavated, the damage zone (FAI ⩾ 2) is mainly located on the left and right side walls. The maximum depth of damage zone is about 3 m, which is located in the middle elevation position of left and right side walls. The area between FAI=1 and 2 is not too large, and the distribution thickness is about 1 m. The test hole results show that the thickness of damage zone is 1.9 m, and the range of damage zone is basically the same as the range of damage zone revealed by the cross-hole acoustic wave monitoring data.

With the passage of time, the area of the damage zone (FAI ⩾2) is relatively stable, and its range basically remains unchanged. The range of failure approach index FAI=1−2 is gradually increasing and becomes stable about 14 days after the excavation is completed. The depths in surrounding rock (that satisfied FAI=1−2) at the positions of centerline of vault, left wall, right wall, and floor that were about 2.5, 6, 5.7, and 4.6 m, respectively. The area of test hole location of FAI ⩾ 1 is basically consistent with the monitoring data of surrounding rock excavation damage zone.

Combined with the test results of excavation damage zone, further analysis shows that the surrounding rock excavation damage zone can be subdivided into yielding zone and failure zone during the time of evolution.

The yield zone can be characterized by FAI⩾1, and its stress state corresponds to the stress state between the peak strength and the residual strength in the rock stress−strain curve. In this area, the expansion of failure zone (FAI ⩾ 2) continues to increase with the passage of time, and gradually stabilizes eventually. The borehole camera results show that there is no obvious macroscopic crack evolution in this area, and it is speculated that the damage of this area should be dominated by microscopic crack expansion based on the weakening law of its acoustic and mechanical properties with time.

The stress state in the failure zone (FAI⩾2) corresponds to the region post residual strength in the rock stress−strain curve. The zone will develop in the form of macro cracks, and the rock mass has already experienced a greater degree of damage.

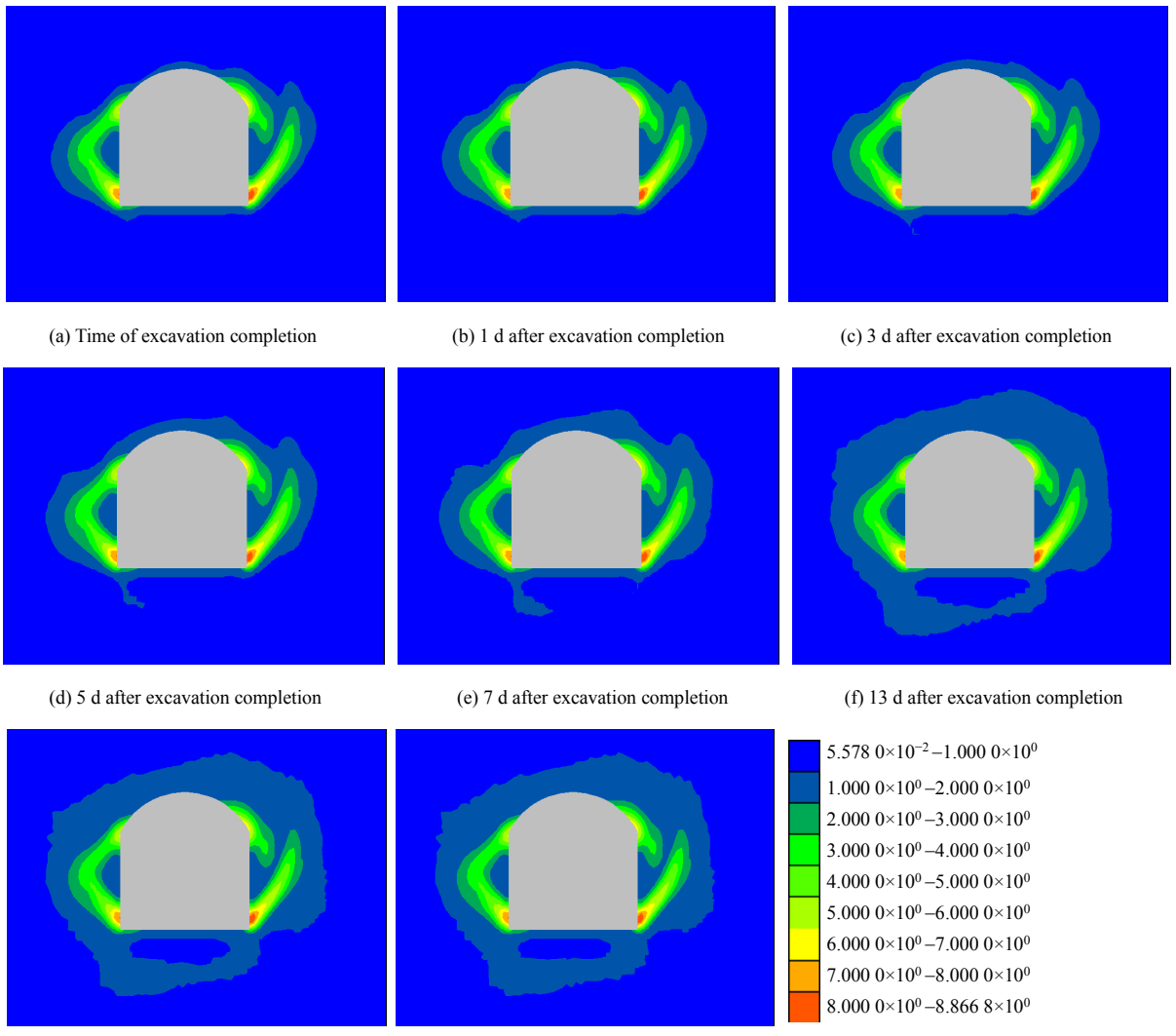

(a) Time of excavation completion (b) 1 d after excavation completion (c) 3 d after excavation completion

(d) 5 d after excavation completion (e) 7 d after excavation completion (f) 13 d after excavation completion

(g) 19 d after excavation completion (h) 25 d after excavation completion

Fig.7 FAI distributions in surrounding rock at different times after excavation

4 Conclusions

(1) In this paper, the LSSVM-PSO intelligent inversion analysis method considering the time-dependent expansion of excavation damage zone is established. Combined with the field monitoring results, this method can obtain the key parameters of the time-dependent rock strength evolution model, and can simulate the time-dependent evolution characteristics of surrounding rock excavation damage zone well.

(2) Under the action of high geostress, the shape of tunnel surrounding rock excavation damage zone is controlled by the state of geostress. The shape of excavation damage zone is approximately a rectangle consistent with the principal stress direction, and the minimum principal stress direction is the main expansion direction of excavation damage zone, the failure zone is also mainly concentrated in this direction.

(3) After the excavation of underground tunnel, the area of excavation damage zone changes approximately in S-shaped curve with time. The initial development is relatively slow, and it tends to increase linearly with time, and finally gradually stabilizes. The period from the 3rd to 10th day is the stage of rapid growth of the damage zone. To a certain extent, it can be explained that after the excavation and unloading energy is released, the surrounding rock will enter a relatively quiet period. As the internal damage of surrounding rock accumulates, the range of surrounding rock excavation damage zone accelerates. The plasticity of the surrounding rock continues to expand and the energy is consumed, until it eventually stabilizes again.

At present, the time-dependent evolution model of rock strength only considers the time-dependent evolution law of rock materials before yield strength. Therefore, the LSSVM-PSO intelligent inversion analysis method developed in this paper also considers only the factors of rock strength and time evolution before yielding. The next step is to make an in-depth study on the evolution law of time-dependent rock strength after yielding.

References

[1] HOEK E, MARTIN C D. Fracure initiation and propagation in intact rock—a review[J]. Journal of Rock Mechanics and Geotechnical Engineering, 2014, 6(4): 287−300.

[2] ZHOU Hui, YANG Yan-shuang, GAO Hong, et al. Experimental investigations on the short-and long-term behaviour of Jinping marble in deep tunnels[J]. European Journal of Environmental and Civil Engineering, 2015, 19(Suppl.1): 83−96.

[3] CUI Guang-Yao, QI Jia-suo, WANG Ming-sheng. Field test study on large deformation control of surrounding rock of cleaved basalt tunnel[J]. Rock and Soil Mechanics, 2018, 39(Suppl. 2): 231, 237, 262.

[4] HAO Xian-jie, FENG Xia-ting, YANG Cheng-xiang, et al. Analysis of EDZ development of columnar jointed rock mass in the Baihetan diversion tunnel[J]. Rock Mechanics and Rock Engineering, 2016, 49(4): 1289−1312.

[5] LI Hai-bo, LIU Ming-chang, XING Wan-bo, et al. Failure mechanisms and evolution assessment of the excavation damage zone in a large scale and deeply buried underground powerhouse[J]. Rock Mechanics and Rock Engineering, 2017, 50(7): 1883−1900.

[6] CHANG Soo-ho, LEE Chung-in, LEE Youn-kyou. An experimental damage model and its application to the evaluation of the excavation of the excavation damage zone[J]. Rock Mechanics and Rock Engineering, 2007, 40(3): 245−285.

[7] LI Shao-jun, FENG Xia-ting, LI Zhan-hai, et al. In situ experiments on width and evolution characteristics of excavation damaged zone in deeply buried tunnels[J]. Science China Technology Science, 2011, 54(Suppl.1): 167−174.

[8] ZHOU Hui, YANG Yan-shuang, LIU Hai-tao. Time-dependent theoretical model of rock strength evolution[J]. Rock and Soil Mechanics, 2014, 35(6): 1521−1527.

[9] ZHANG Chuan-qing, ZHOU Hui, FENG Xia-ting, et al. Stochastic analysis method on safety of surrounding rock mass based on yielding approach index[J]. Chinese Journal of Rock Mechanics and Engineering, 2007, 26(2): 292−299.

[10] ZHANG Chuan-qing, ZHOU Hui, FENG Xia-ting. Stability assessment of rockmass engineering based on failure approach index[J]. Rock and Soil Mechanics, 2007, 28(5): 888−894.

[11] GAO Shang, YANG Jing-yu. Swarm intelligence algorithm and its application[M]. Beijing: China Water and Hydropower Press, 2006.

[12] ZHAO Tong-bin, TAN Yun-liang, LIU Chuan-xiao. Research on back-analysis of roadway displacement based on genetic algorithms[J]. Rock and Soil Mechanics, 2004, 25(Suppl.1): 107−109.